ISSN 1023-1935, Russian Journal of Electrochemistry, 2008, Vol. 44, No. 8, pp. 910–920. © Pleiades Publishing, Ltd. 2008.
Original Russian Text © Yu.G. Chirkov, V.I. Rostokin, 2008, published in Elektrokhimiya, 2008, Vol. 44, No. 8, pp. 981–991.

Fuel Cell Cathode with Nafion and Platinum: Calculating its Overall Performance with Consideration of Gas- and Vapor-Exchange Processes in the Gas-Diffusion Layer

Yu. G. Chirkov[a,z] and V. I. Rostokin[b]

[a] *Frumkin Institute of Physical Chemistry and Electrochemistry, Russian Academy of Sciences, Leninskii pr. 31, Moscow, 119991 Russia*

[b] *Moscow Institute of Engineering Physics, Kashirskoe sh. 31, Moscow, 117409 Russia*

Received March 19, 2007

Abstract—The overall performance of cathodes with solid polymer electrolytes is calculated for three different cases in which gas- and vapor-exchange processes in the gas-diffusion layer are considered. First of all, specific results are presented for calculating the overall performance of oxygen and air cathodes under the assumption that external diffusion restrictions are completely absent. Then with these same conditions (i.e., all the parameters characterizing the active layer of the cathode remain the same), results of the overall performance are given for the idealized case in which gas exchange in the gas-diffusion layer causes the appearance of limiting currents, but in this case vapor exchange is completely ignored. Finally, an analysis is carried out to determine how vapor-exchange processes in the gas-diffusion layer alter overall cathode performance and what measures should be taken to reduce the significance of external diffusion restrictions.

Key words: fuel cell with Nafion membrane, gas-diffusion layer, Stefan flows, Darcy's law, gas and vapor exchange, limiting currents

DOI: 10.1134/S1023193508080053

INTRODUCTION

In order to achieve high values of conductivity of the solid polymer electrolyte in fuel cells with Nafion, optimal conditions for its humidification must be maintained. Different approaches for this have been proposed, but saturation of the reactant gases with water vapor is the most common [1]. In this case the temperature of the vapor must be higher than that of the fuel cell. For example, Ticianelli et al. [2] recommend raising the temperature of the oxygen or air cathode by5°C and that of the hydrogen anode by 10°C. Our goal in this work is to perform a qualitative and quantitative analysis of how gas humidification in the oxygen or air cathode of a fuel cell with Nafion affects its overall performance.

GAS-DIFFUSION LAYER: MATHEMATICAL FORMULAS

Let us examine the mathematical apparatus that enables us to calculate the overall performance of a cathode with Nafion when gas- and vapor-exchange processes occur in the gas-diffusion layer.

Figure 1 shows a schematic diagram of the fuel-cell units, which are operationally and directly in contact with the active layer (AL) of the cathode: the gas chamber (GC), the gas-diffusion layer (GDL), and the Nafion membrane (M). Water vapor can either be released toward the surface of the active layer (membrane humidification) or released from the active layer (membrane drying). A mixture of either oxygen and water vapor

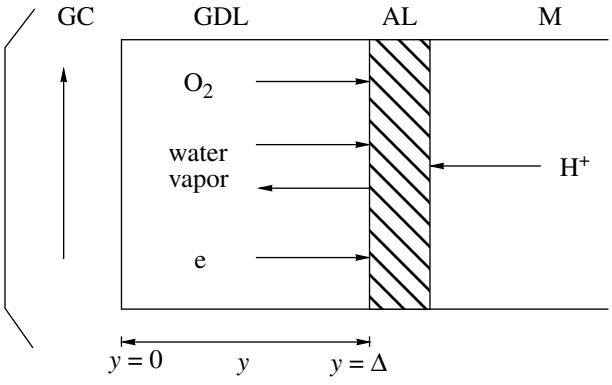

Fig. 1. Schematic diagram of fuel-cell components, which are operationally and directly in contact with the active layer (AL) of the cathode: gas chamber (GC), gas-diffusion layer (GDL), and fuel-cell membrane (M).

[z] Corresponding author, e-mail: olga.nedelina@gmail.com

(oxygen cathode) or oxygen, nitrogen, and water vapor (air cathode) can be admitted into the gas chamber.

In this section of the paper we will examine only processes that occur in the gas-diffusion layer. The following interpretation of the phenomena is usually assumed in the literature. It is well known that if an electrochemical (heterogeneous) reaction is accompanied by a decrease in the volume of the reacting mixture (the rear surface of the active layer in Fig. 1), then the total flow of the reacting mixture (nitrogen with oxygen and water vapor) originates in the direction normal to the surface at which the reaction occurs [3]. Thus, Stefan flows of the gas–vapor mixture originate at the cathode [4, 5].

It is usually assumed that filtration flows of gases, which are caused by a pressure difference, significantly exceed Stefan flows in porous membranes [6]. Therefore, to a first approximation, it is possible to assume that the total pressure of the gaseous mixture is constant (the total gas pressure quickly adjusts itself); i.e., the following equation is satisfied: $p + p_N + p_w = 1$, where these three quantities are the reduced partial pressures of oxygen, nitrogen, and water vapor, respectively (they are divided by the total pressure p^* of the gases and water vapor in the gas chamber). In this work we will examine the general case of the operation of the gas-diffusion layer when the total gas pressure in it is not constant across the thickness of the layer and the inequality $p + p_N + p_w \neq 1$ is the case.

Stefan flows of oxygen, hydrogen, and water vapor have the form

$$-\mathrm{d}p/\mathrm{d}\ddot{y} + \mathring{u}p = \bar{I}, \quad (1)$$

$$-\mathrm{d}p_N/\mathrm{d}\ddot{y} + \mathring{u}p_N = 0, \quad (2)$$

$$-\mathrm{d}p_w/\mathrm{d}\ddot{y} + \mathring{u}p_w = \bar{I}_w, \quad (3)$$

where $\ddot{y} = y/\Delta$ is the reduced coordinate, which is directed perpendicularly from the GDL to the active layer (Fig. 1); Δ is the thickness of the gas-diffusion layer; $\mathring{u} = u/u^*$ is the reduced bulk (molar) velocity of the flow of the gas–vapor mixture; $u^* = D^{**}/\Delta$ is the characteristic velocity; D^{**} is the effective diffusion coefficient of the gas–vapor mixture; $\bar{I} = I/I_d$ is the reduced current in which the characteristic diffusion current $I_d = nFD^{**}p^*/RT\Delta = (nFD^{**}p_0^*/RT\Delta)\varepsilon = I_p^*\varepsilon$, where $\varepsilon = p^*/p_0^*$, with $p_0^* = 101$ kPa; and $\bar{I}_w = nFI_w/I_d$ is the reduced water-vapor flow.

The formulation of the problem demands a statement of boundary conditions at the gas-diffusion layer, and these have the form

$$\ddot{y} = 0 \quad p = p_0 \quad p_N = p_{N0} \quad p_w = p_{w0}, \quad (4)$$

$$\ddot{y} = 1 \quad p = p_s \quad p_N = p_n \quad p_w = p_{w1}, \quad (5)$$

where p_0, p_{N0}, and p_{w0} are the reduced partial pressures of oxygen, nitrogen, and water vapor, respectively, in the gas chamber, and p_s, p_n, and p_{w1} are the reduced partial pressures of oxygen, nitrogen, and water vapor, respectively, at the boundary between the active and gas-diffusion layers. Of these six pressure quantities, the first three are assigned parameters for the problem and can serve as boundary conditions for Eqs. (1)–(3). The other three quantities are initially unknown and must be determined in the course of calculating the distribution of partial pressures across the thickness of the gas-diffusion layer and matching values for the functions p, p_N, and p_w with the functions that characterize the active layer of the cathode (the representation of oxygen supersaturation of Nafion at the boundary between the active and gas-diffusion layers).

For a better general description of the processes occurring in the gas-diffusion layer, we must supplement the system of Stefan flows of oxygen, nitrogen, and water vapor in Eqs. (1)–(3) with Darcy's equation,

$$U = -(\tau p^*/\mu)\mathrm{d}(p + p_N + p_w)/\mathrm{d}y, \quad (6)$$

where U is the mass velocity of the gas flow; τ is the permeability of the gas-diffusion layer; and μ is the viscosity of air. Darcy's equation contains the mass velocity U rather than the bulk (molar) velocity. These two quantities would be equal to each other if the molar masses of all the components of the gas–vapor mixture were the same. The molar mass of oxygen ($M_{O_2} = 32$) is approximately equal to that of nitrogen ($M_{N_2} = 28$), but differs significantly from the molar mass of water ($M_{H_2O} = 18$). However, in order not to further complicate the already rather cumbersome system of equations under study, we will first assume that $u = U$. Then Darcy's equation can be rewritten in the form

$$\mathring{u} = -\alpha\mathrm{d}(p + p_N + p_w)/\mathrm{d}\ddot{y}. \quad (7)$$

This equation contains the basic parameter of the problem, the ratio of the characteristic filtration rate of the gas to its diffusion velocity, $\alpha = \tau p^*/D^{**}\mu = (\tau p_0^*/D^{**}\mu)\varepsilon = \alpha^*\varepsilon$. Thus, the parameter α can be represented as the product of two quantities: a structural component α^*, which is determined by the properties of the gas-diffusion layer, and a "barometric" component ε, which depends on the total pressure in the gas chamber.

Since there are five quantities to be determined, including the functions p, p_N, p_w, and $\mathring{u}$, which depend on the coordinate y, along with the constant p_n, we must add another condition, which fulfills the continuity equation [7], to the system of Eqs. (1)–(3) and (7):

$$\mathrm{d}[\mathring{u}(p + p_N + p_w)]/\mathrm{d}\ddot{y} = 0. \quad (8)$$

Let us now find the general solution to the system of Eqs. (1)–(3), (7), and (8) with the conditions in Eqs. (4) and (5).

We will introduce the notation $\Sigma = p + p_N + p_w$. Then adding together Eqs. (1)–(3), we have

$$-d\Sigma/d\ddot{y} + \mathring{u}\Sigma = \bar{I} + \bar{I}_w, \quad (9)$$

and in place of Eqs. (7) and (8) we obtain

$$\mathring{u} = -\alpha d\Sigma/d\ddot{y}, \quad (10)$$

$$d(\mathring{u}\Sigma)/d\ddot{y} = 0. \quad (11)$$

Eqs. (9)–(11) are supplemented by the conditions

$$\ddot{y} = 0 \quad \Sigma = 1, \quad (12)$$

$$\ddot{y} = 1 \quad \Sigma = \Sigma_1 = p_s + p_n + p_{w1}. \quad (13)$$

Eliminating the velocity $\mathring{u}$, from Eqs. (9)–(11), we obtain the two differential equations:

$$-d\Sigma/d\ddot{y} - \alpha\Sigma d\Sigma/d\ddot{y} = \bar{I} + \bar{I}_w, \quad (14)$$

$$d(\Sigma d\Sigma/d\ddot{y})/d\ddot{y} = 0. \quad (15)$$

Integrating Eq. (14) in conjunction with the conditions in Eqs. (12) and (13), we have

$$\bar{I} + \bar{I}_w = 1 - \Sigma_1 + \alpha(1 - (\Sigma_1)^2)/2, \quad (16)$$

Thus, integrating Eq. (15) in conjunction with the same two conditions, we find the distribution of the sum of the partial pressures Σ through the thickness of the gas-diffusion layer:

$$\Sigma = \{1 - [1 - (\Sigma_1)^2]\ddot{y}\}^{1/2}. \quad (17)$$

Now with Eq. (10), we can determine the velocity $\mathring{u}$:

$$\mathring{u} = \alpha[1 - (\Sigma_1)^2]/2\{1 - [1 - (\Sigma_1)^2]\ddot{y}\}^{1/2} = (\alpha\beta/2)/\{1 - \beta\ddot{y}\}^{1/2}, \quad (18)$$

where $\beta = 1 - (\Sigma_1)^2$. Equation (18), in turn, makes it possible to integrate Eq. (2), and this leads to

$$p_n = p_{N0}\exp[\alpha(1 - \Sigma_1)]. \quad (19)$$

Equations (16) and (19) enable us to determine completely the sum of the flows $\bar{I} + \bar{I}_w$ in the system being studied.

Let us now determine the quantities $\bar{I}$ and $\bar{I}_w$ separately. In order to determine the current $\bar{I}$, we need to integrate Eqs. (1) and (3) in conjunction with the expression in Eq. (18). As a result, we have

$$p = \{C + \bar{I}(2/\alpha^2\beta)[\alpha(1 - \beta\ddot{y})^{1/2} - 1] \times \exp[\alpha(1 - \beta\ddot{y})^{1/2}]\}\exp[-\alpha(1 - \beta\ddot{y})^{1/2}], \quad (20)$$

$$p_w = \{C_2 + \bar{I}_w(2/\alpha^2\beta)[\alpha(1 - \beta\ddot{y})^{1/2} - 1] \times \exp[\alpha(1 - \beta\ddot{y})^{1/2}]\}\exp[-\alpha(1 - \beta\ddot{y})^{1/2}]. \quad (21)$$

Using the conditions in Eqs. (4) and (5) to eliminate the integration constants C and C_2 from Eqs. (20) and (21), we obtain

$$\bar{I} = \alpha^2\{[1 - (\Sigma_1)^2]/2\}[p_0\exp\alpha - p_s\exp(\alpha\Sigma_1)]/[(\alpha - 1)\exp\alpha - (\alpha\Sigma_1 - 1)\exp(\alpha\Sigma_1)], \quad (22)$$

$$\bar{I}_w = \alpha^2\{[1 - (\Sigma_1)^2]/2\}[p_{w0}\exp\alpha - p_{w1}\exp(\alpha\Sigma_1)]/[(\alpha - 1)\exp\alpha - (\alpha\Sigma_1 - 1)\exp(\alpha\Sigma_1)]. \quad (23)$$

Equations (19), (22), and (23) completely determine the overall current $\bar{I}$ and the flow of water vapor $\bar{I}_w$. The partial pressures of the saturated water vapor in the gas chamber p_{w0} and at the boundary between the active and gas-diffusion layers p_{w1} are defined by the temperature of the saturated water vapor in the gas chamber and the working temperature of the fuel cell. We further note that the requirement of matching the solutions obtained for the active and gas-diffusion layers assumes that an additional condition be fulfilled. Indeed, oxygen solubility in Nafion c_s at the boundary between the active and gas-diffusion layers depends on the pressure and is presented in the form

$$c_s = p_s. \quad (24)$$

Two limiting cases, the oxygen cathode and the air cathode, represent the greatest practical interest.

Oxygen Cathode

For all the formulas in this case, the partial pressure of nitrogen p_N is identically zero, so $\Sigma_1 = p_s + p_{w1}$.

Under steady-state conditions for the operation of the cathode, ideally it would be necessary to carry off the flow of vapor from the gas chamber, not only the water formed in the active layer of the cathode $\bar{I}$, but also the moisture, which the proton flow carries with it in the membrane $\gamma\bar{I}$. Therefore, for the water balance, it would be necessary to have

$$-\bar{I}_w = \bar{I}(1+\gamma), \quad (25)$$

where the parameter $\gamma > 0$. It is clear that under conditions of gas humidification in the cathode compartment (in this case, $\bar{I}_w > 0$) the condition in Eq. (25) cannot be fulfilled. Thus, for steady-state moisture exchange to be established in the cathode under conditions of gas humidification, the filtration flows of water must still occur through GDL pores in the direction from the active layer toward the GDL. The condition in Eq. (25) can be fulfilled only under conditions of the drying of the active layer of the cathode, when the vapor flow is sufficiently strong and directed into the gas chamber (in this case, $\bar{I}_w < 0$).

Air Cathode

In this case, according to Eq. (13), $\Sigma_1 = p_s + p_n + p_{w1}$. The condition in Eq. (19), written in the form

$$p_n = [4(1 - p_{w0})/5]\exp[\alpha(1 - \Sigma_1)]. \quad (26)$$

enables us to determine the additional quantity p_n.

In conclusion we need to make the following observation. In the general case, the gas pressure at the boundary between the active and the gas-diffusion layers (designated as p^{**}) is less than the gas pressure in the gas chamber (p^*). It is obvious that $p^{**} = p^*\Sigma_1$. Therefore, the overall current in the active layer of the cathode no longer increases in proportion to $(p^*)^{1/2}$ (the case when the gas-diffusion layer does not introduce any restrictions to current generation in the active layer), but is proportional to the smaller quantity $(p^{**})^{1/2} = (p^*)^{1/2}(\Sigma_1)^{1/2}$.

OVERALL CATHODE CHARACTERISTICS WITHOUT CONSIDERATION OF VAPOR EXCHANGE

Let us now proceed to calculations. Our ultimate goal is to demonstrate how gas and vapor exchange in the gas-diffusion layer affects overall performance of a cathode with Nafion and platinum. With several values of gas pressure in the gas chamber, we will first calculate current–voltage curves for the oxygen and air cathodes under the conditions that external diffusion restrictions are completely absent. Next we will examine a cathode with a gas-diffusion layer in which there is gas exchange (flows of oxygen and nitrogen if this is an air cathode), but in this case we will again assume that vapor flows are negligible. As a result, the role of gas exchange in the gas-diffusion layer in leading to the development of limiting currents in the cathode will be established.

Let us begin a solution to the first problem, the calculation of cathode performance for the ideal case that external diffusion losses are completely absent. It is apparent that in this case the characteristics contributing to the overall cathode performance achieve their maximum possible values. In order to perform such calculations, we must first choose structural parameters for the active layer, parameters that characterize the electrochemical process of oxygen reduction on platinum, and also specify the external conditions under which the active layer of the cathode operates.

External Parameters

Let the working temperature be t = 80°C and the thickness of the active layer of the cathode be Δ_1 = 10 μm. The pressure in the gas chamber p^* will have three values: 101, 303, and 505 kPa.

Parameters of Electrochemical Kinetics

For oxygen reduction on platinum in acidic media, two slopes of the Tafel curve are observed: 0.06 V (the region of large potentials) and 0.12 V (region of small potentials) [8–11]. Overall currents and other characteristics of the active layers of cathodes with Nafion and platinum must be calculated when polarization curves of the catalyst have two or more segments with different slopes and exchange currents, as we showed previously [12].

We will choose E-TEK (XC72 + 20 mass % Pt) as the catalyst. Let us assume that the steady-state potential of the cathode is E_{st} = 1.05 V, that the potential of the inflection point on the Tafel curve is E^* = 0.825 V, that the slopes of the Tafel curve are $b_1 = 2.6 \times 10^{-2}$ V (in the region of high potentials) and $b_2 = 5.2 \times 10^{-2}$ V, and that the number of electrons participating in the reaction is n = 4. We will also assume that the exchange current at t = 50°C is $i_o = 10^{-8}$ A/cm^2 [13]. The temperature dependence of electrode kinetics (exchange current) for oxygen reduction on platinum is given by $i_0 = i_0^{ref}\exp[8804\,(1/T_{ref} - 1/T)]$ [14]. For the change from 50°C to the fuel cell temperature of t = 80°C, the exchange current increases to a value of $i_o = 10^{-7}$ A/cm^2.

The mathematical formulas for determining the overall performance of the active layer of a cathode with Nafion contain four parameters: the effective diffusion coefficient D^*, the effective specific conductivity κ^*, the oxygen solubility in Nafion c_0, and the characteristic bulk current density i^* [15]. Calculation of the effective diffusion coefficient D^* and the effective conductance κ^* requires knowledge of structural parameters for the active layer.

Structural Parameters of the Active Layer

It is usually assumed that the size of the carbon-black particles is ~ 20–40 nm, that agglomerates of these particles (grains of the carrier) vary in size from tens to hundreds of nanometers, that pores between agglomerates are located in that size range, and that they are partially filled with agglomerates of molecules of the solid polymer electrolyte (grains of Nafion) [16].

Let us assume, as we did previously [17], that the structure of the active layer can be described with the "model of equidimensional grains," in which all the grains have the form of identical microcubes with an edge length of L. All these grains are closely packed, so their centers form a regular cube of "lattice points." There are three types of grains: those of the carrier (carbon black) with the catalyst (platinum) deposited on them, their volume fraction designated as g_s; those of Nafion (agglomerates of Nafion molecules), their volume fraction designated as g_e; and "grains" of void space, their volume fraction designated as g_0.

We have previously analyzed how the structure of the active layer (the sum of the values of g_s, g_e, and g_0 is unity) influences the effectiveness of the processes taking place within it [18]. It was shown that the active layer operates normally only in the interval $0.31 \le g_e \le (0.69 - g_0)$. For $g_e < 0.31$, there is insufficient material for the formation of an ionic percolation cluster, the supply channel to the zone where an ionic current (protons) is generated, while for $g_e > (0.69 - g_0)$, there are no conditions for the existence of an electron percolation cluster, the channel for supplying electrons and gas (oxygen).

One feature of cathodes with Nafion is that an electrochemical process can occur in them only where grains leading to an ionic cluster come in direct contact with grains leading to an electron cluster. It is clear that as the concentration of voids increases in the active layer, the specific contact surface between ionic and electron clusters (we will designate this surface as S^*) rapidly decreases. The boundaries of the region in which the surface S^* and the current are nonzero also shrink. Therefore, in our calculations, we will assume that $g_0 = 0$, i.e., that there are no voids in the active layer. This is not such a bad assumption since in reality grains of Nafion and the carrier can significantly differ in form and size [16]. It is reasonable to assume that there is sufficiently close packing of grains of Nafion with those of the carrier in the active layer for the volume fraction due to voids to be considered negligible.

We have shown that the maximum value of S^* is reached when the volume concentrations of grains of Nafion and those of the carrier are equal to each other, i.e., $g_e = g_s = 0.5$ [18]. Then the value of S^* can be determined from the formula $S^* = 1.33/L$. We will assume that grain size is $L = 100$ nm, that pore size in grains of the carrier is $d = 30$ nm, and that the porosity of grains of the carrier is $\nu = 0.5$.

In the absence of voids in the active layer, oxygen can enter the zone of current generation mainly through small pores in grains of the carrier, which lead to the structure of the electron cluster. In pores with a diameter of 30 nm there is Knudsen flow of the gas, and studies suggest that the coefficient of such diffusion is $D_{kn} = 4 \times 10^{-3}$ cm^2/s. However, gas moves in the active layer through grains of the carrier leading to a percolation cluster, which has a complex fractal structure. Therefore, as we have shown in our percolation calculations, the effective diffusion coefficient in the active layer turns out to be smaller by approximately an order of magnitude and has an exact value of $D^* = 4.5 \times 10^{-4}$ cm^2/s [17]. Similar considerations can be expressed about proton movement in an ionic cluster. Although the optimal specific conductivity of Nafion is $\kappa = 1 \times 10^{-1}$ S cm^{-1}, its effective specific conductivity in the active layer turns out to be an order of magnitude smaller, with an exact value of $\kappa^* = 1.09 \times 10^{-2}$ S cm^{-1}.

Further, we will take oxygen solubility, which depends on the pressure according to Henry's law, in Nafion as $c_o = 5 \times 10^{-6}\,\varepsilon$ g-mol/cm^3 [19]. At a pressure of $p^* = 505$ kPa, for example, the parameter $\varepsilon = 5$, the solubility is $c_o = 2.5 \times 10^{-5}$ g-mol/cm^3.

Now it remains to determine the value of the characteristic bulk current density i^* in the region of high potentials. It is the product of the exchange current i_0 in the region of high potentials and the specific surface S of the particles of the catalyst (platinum), which are available to participate in the electrochemical process in a unit volume of the active layer of the cathode. Thus, $i^* = i_0 S$.

The specific surfaces S and S^* are not the same of course. The fact is that the surface "contact" between grains of the ionic and electron clusters is not flat, but rather as if it were eroded to some depth. Both Nafion molecules carbon-black particles with the catalyst exist in this region of surface contact between the grains. In estimating values of the surface S, we considered a number of points. First of all, as noted above, the active layer does not consist of identical grains in reality. Therefore, we chose a value of 100 nm for L, which is larger than the intermediate value (between tens and hundreds of nanometers [16]). Secondly, it is necessary to consider that not the entire external surface of grains of the carrier (agglomerates of carbon-black particles) is catalytically active. Therefore, it seems reasonable to estimate S according to the formula $S = S^*\xi$, where ξ is the catalytically active fraction of the surface of grains of carrier.

Thus, $i^* = i_0 S^*\xi = 1.33\, i_0\, \xi/L$. If we assume that $\xi = 0.6$, the specific surface of the electrochemically active platinum in the active layer of the cathode with Nafion is $S = 8 \times 10^4$ cm^{-1}, and the characteristic bulk current density in the region of high potentials is $i^* = 8$ mA/cm^3. It is necessary to emphasize that the value obtained for i^* is only an estimate. This value and the other parameters we have chosen for the active layer of the cathode with Nafion and platinum remain the same in all of the following calculations.

Let us now proceed to the results of calculations of the overall performance.

CATHODE WITH NAFION AND PLATINUM WITHOUT EXTERNAL DIFFUSION RESTRICTIONS

Figure 2 presents current–voltage curves (*1*–*3*) and the specific power W of the fuel cell as a function of overall current (*1'*–*3'*) for three values of gas pressure p^* in the gas chamber (101, 303, and 505 kPa) of the air and oxygen cathodes. In performing calculations of specific power, we have considered the hydrogen–oxygen (air) fuel cell with Nafion and platinum and assumed that the overvoltage at the anode is negligible in comparison to that at the cathode. Thus, the voltage of the fuel cell is equal to the cathode potential. In this case, we apparently ought to obtain a low estimate for the value of the specific power. In addition, it was

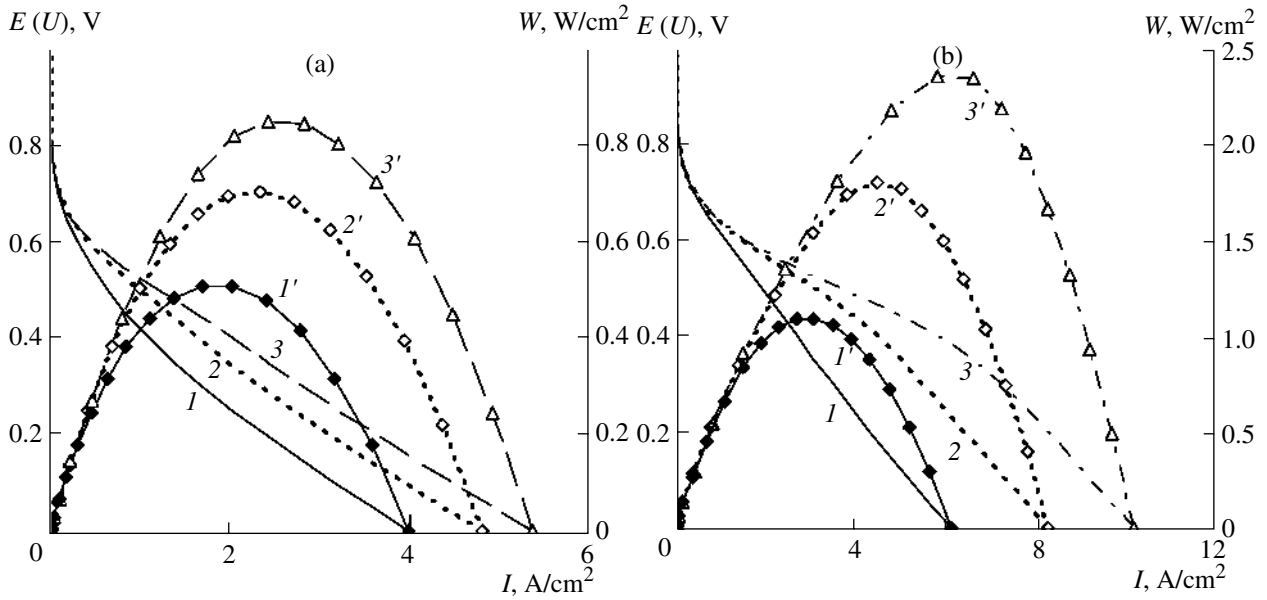

Fig. 2. Current–voltage curves of the cathode (*1–3*) and specific power of a fuel cell as a function of overall current (*1′–3′*) for (a) air and (b) oxygen cathodes without any restrictions on gas and vapor exchange in the gas-diffusion layer. The temperature of the fuel cell is*t* = 80°C; the thickness of the active layer is Δ_1 = 10 μm; and the pressure p^* in the gas chamber (in kPa) is *1*, *1*′ – 101; *2*, *2*′ – 303; and *3*, *3*′ - 505.

assumed that the thickness of the membrane is Δ_2 = 10 μm and that the specific conductivity of Nafion in the membrane is $\kappa = 1 \times 10^{-1}$ S cm^{-1}.

Figure 2 shows that up to a potential of E= 0.7 V the overall current and specific power are nearly independent of the gas pressure p^* in the gas chamber. This dependence and internal diffusion restrictions develop only at potentials of $E > 0.7$ V (divergence of curves *1–3*). At p^* = 101 kPa, the overall current reaches approximately 1 A/cm^2 for the oxygen cathode at E = 0.6 V and for the air cathode at E = 0.4 V. Consequently, the specific power reaches values on the order of 1 W/cm^2 for the oxygen cathode and 0.4 W/cm^2 for the air electrode.

The data in Fig. 2 is of interest not only for itself. It provides reference values for further analysis; they are the maximum values capable of giving rise to the active layer of a cathode with Nafion in the complete absence of restrictions in the gas-diffusion layer. These values will be compared with I and W obtained in the presence of external diffusion restrictions, at first gas exchange, but then with the addition of vapor exchange.

CATHODE WITH NAFION AND PLATINUM WITH CONSIDERATION OF GAS DIFFUSION IN THE GAS-DIFFUSION LAYER

Let us proceed to the second point of the calculations, the consideration of gas exchange in the gas-diffusion layer, but we will ignore vapor-exchange processes. Formally, this means that the vapor pressure is set identically equal to zero in the formulas, i.e., $p_w \equiv 0$.

The influence of gas exchange on the overall performance of the cathode with Nafion and platinum for oxygen and air cathodes has been analyzed previously in considerable detail [20]. Therefore, here we will only cite the results of the calculations, which we performed. The potential (voltage) and specific power are shown in Fig. 3 as functions of the overall cathode current of the fuel cell for the same three values of gas pressure in the gas chamber for air and oxygen cathodes, as in Fig. 2. The characteristic diffusion current I_α^* = 1.035 A/cm^2 and the parameter λ^* = 0.156 were chosen as the basic characteristics of the gas-diffusion layer. We have previously provided our rationale for choosing these two particular values [20].

The presence of restrictions on the oxygen supply in the gas-diffusion layer causes the appearance of limiting currents. In the absence of gas-diffusion restrictions in the oxygen electrode, the saturation of Nafion with oxygen at the boundary between the active and gas-diffusion layers is independent of the potential and has a value of unity (c_s = 1). In the air electrode the saturation is c_s = 0.2. The situation is different if gas exchange takes place in the gas-diffusion layer. In this case the value of c_s becomes dependent on the potential. From the condition of equal oxygen flows in the gas-diffusion and active layers, it follows that as the potential decreases, the overall current can increase only through a decrease in c_s. This quantity can decrease to zero, and as c_s tends toward zero, it indicates that the overall current is gradually moving toward its limiting value.

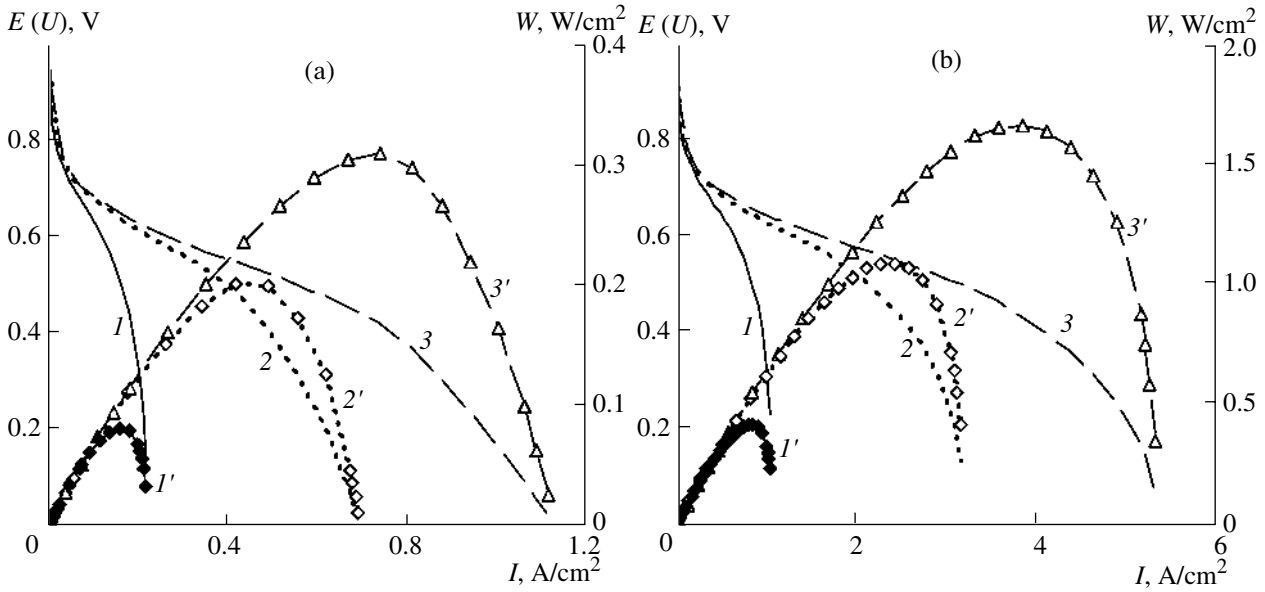

Fig. 3. Current–voltage curves of the cathode (*1–3*) and specific power of a fuel cell as a function of overall current (*1'–3'*) for (a) air and (b) oxygen cathodes with restrictions on the oxygen supply in the gas-diffusion layer and the complete neglect of vapor-exchange processes. The temperature of the fuel cell is $t = 80°C$; the thickness of the active layer is $\Delta_1 = 10$ μm; and the pressure p^* in the gas chamber (in kPa) is *1*, *1'* – 101; *2*, *2'* – 303; and *3*, *3'* – 505. $I_d^* = 1.035$ A/cm^2, and $\alpha* = 0.156$.

It is worth noting further that at a pressure of $p^* = 101$ kPa the limiting current for the oxygen cathode reaches approximately 1 A/cm^2 since, according to the conditions of the calculations, $I_d^* = 1.035$ A/cm^2. A comparison of Figs. 2 and 3 shows that the specific power decreases markedly. For the air cathode at a pressure of $p^* = 101$ kPa, the limiting current reaches a value of approximately 0.2 A/cm^2. As Fig. 2 shows, the limiting current and specific power rise significantly, increasing the gas pressure in the gas chamber.

Table 1. Current I and specific power W of a fuel cell with Nafion and platinum, the reduced oxygen pressure p_s at the boundary between the active and gas-diffusion layers, and the water-vapor flow I_w in the gas-diffusion layer as functions of the cathode potential E and the pressure p^* in the gas chamber (The oxygen cathode is at $t = 80°C$; the vapor temperature at the entrance to the gas chamber is $t^* = 95°C$; and the thickness of the active layer is 10 μm)

p^*, kPa	E, V	I, A/cm^2	W, W/cm^2	$p_s = c_s$	I_w, A/cm^2
101	0.78	0.016	0.012	0.16	0.404
	0.69	0.057	0.039	0.12	0.408
	0.60	0.108	0.065	0.07	0.413
	0.48	0.148	0.071	0.03	0.417
	0.29	0.172	0.051	0.006	0.419
	0.18	0.176	0.031	0.002	0.419
505	0.77	0.105	0.081	0.85	0.079
	0.70	0.357	0.249	0.82	0.082
	0.59	1.326	0.781	0.70	0.094
	0.50	2.446	1.223	0.55	0.109
	0.43	3.131	1.335	0.45	0.118
	0.31	3.764	1.153	0.35	0.128

OVERALL CATHODE PERFORMANCE WITH CONSIDERATION OF VAPOR EXCHANGE

With the same assumptions as above (identity of the characteristics of the active layer), the results of calculating the overall cathode performance under conditions that consider both gas and vapor exchange in the gas-diffusion layer are presented. For a concrete example, we will examine the humidification of the active layer. This means that water-vapor flows from the gas chamber move toward the active layer (Fig. 1). It is possible to moisten the active layer if the temperature of the saturated vapor that is fed into the gas chamber is higher than that of the saturated vapor in the active layer of the fuel cell.

An increase in the excessive degree of gas humidity in the gas chamber of the cathode is intended to create optimal conditions for the operation of the Nafion membrane, for increasing its proton conductivity to a value of the order of $\kappa = 1 \times 10^{-1}$ S cm^{-1}. As before, let us assume that the temperature of the fuel cell is $t = 80°C$, but we knowingly choose an excessive value of $t^* = 95°C$ as the temperature of the saturated vapor in the gas chamber.

The results of calculations, which take into account vapor exchange for air and oxygen cathodes with

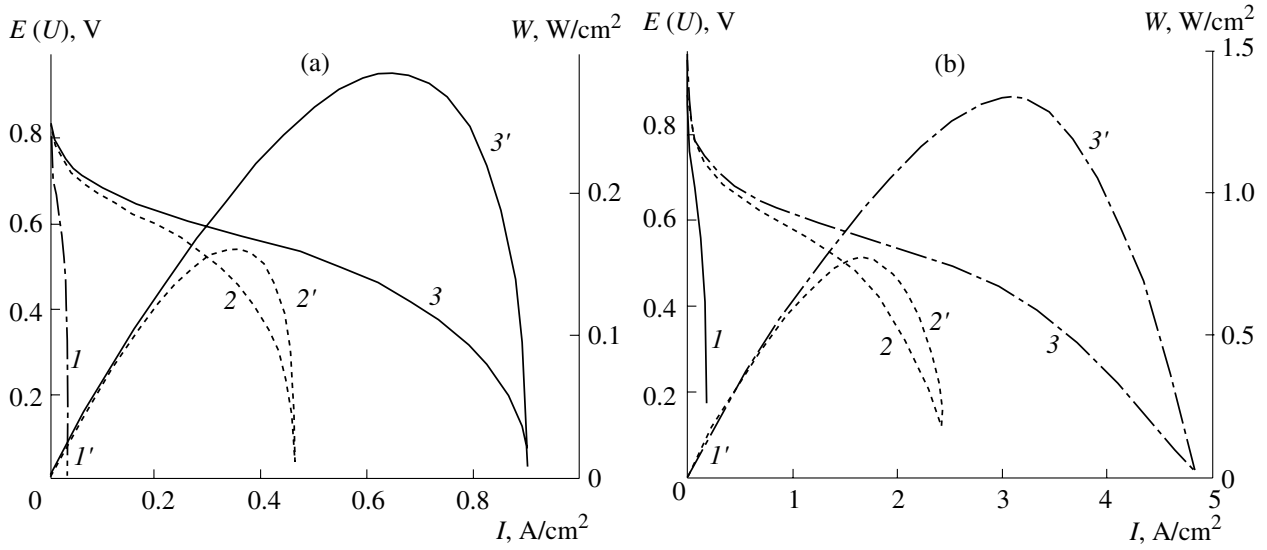

Fig. 4. Current–voltage curves of the cathode (*1*–*3*) and specific power of a fuel cell as a function of overall current (*1*'–*3*') for (a) air and (b) oxygen cathodes with consideration of both gas- and vapor-exchange processes in the gas-diffusion layer. The temperature of the fuel cell is $t = 80°C$; the temperature of saturated vapor at the entrance to the gas chamber is $t^* = 95°C$; the thickness of the active layer is $\Delta_1 = 10$ μm; and the pressure p^* in the gas chamber (in kPa) is *1*, *1*' – 101; *2*, *2*' – 303; and *3*, *3*' – 505. $I_d^* = 1.035$ A/cm^2, and $m\alpha^* = 0.156$.

Nafion and platinum, are shown in Fig. 4 as current–voltage curves (curves *1*–*3*) and specific power of the fuel cell as a function of the overall current (curves *1*'–*3*'). The set of values of *I*, *E*-, and *W* for oxygen and air cathodes are also given in Tables 1 and 2, respectively. All the parameters of the active and gas-diffusion layers are the same as those chosen previously.

Let us now compare Figs. 3 and 4. Excess humidification of the gases entering the gas chamber leads to a significant decrease in the limiting overall currents (curves *1*–*3*). This decrease is especially large at a pressure of $p^* = 101$ kPa and becomes less noticeable with increasing pressure in the gas chamber. An explanation of this phenomenon follows.

Because of the small value of the parameter $\alpha*$ ($\alpha* = 0.156$) and the rather small pressure changes in the gas chamber (from 101 to 505 kPa), filtration flows do not play a significant role in the gas-diffusion layer (in this case the inequality $\alpha* \geq 1$ must be satisfied), but diffusion flows do. Thus, the critical value for current generation in the active layer is the oxygen pressure in the gas chamber. In the gas chamber for $\varepsilon = 1$ ($p^* = 101$ kPa) and at $t^* = 95°C$, the vapor pressure $p_{w0} = 84.5$ kPa. At the boundary between the active and gas-diffusion layers at $t = 80°C$, the vapor pressure $p_{w1} = 47.3$ kPa. Therefore, vapor flow is directed from the gas chamber toward the active layer. Furthermore, for the oxygen cathode, the partial pressure of oxygen in the gas chamber is no longer $p_0 = 1.0$ (dry oxygen, data in Fig. 2b), but $p_0 = (101 - 84.5)/101 = 0.163$. Consequently, the partial pressure of vapor in the gas chamber is $p_{w0} = 0.837$, while the partial pressure of vapor at the active layer is $p_{w1} = 0.467$. The small value of the partial pressure of oxygen in the gas chamber, which is caused by the elevated humidification of the oxygen, leads to a sharp decrease in the diffusion flow of oxygen toward

Table 2. Current *I* and specific power *W* of a fuel cell with Nafion and platinum, the reduced oxygen pressure p_s at the boundary between the active and gas-diffusion layers, and the water-vapor flow I_w in the gas-diffusion layer as functions of the cathode potential *E* and the pressure $p*$ in the gas chamber (The air cathode is at $t = 80°C$; the vapor temperature at the entrance to the gas chamber is $t* = 95°C$; and the thickness of the active layer is 10 μm)

p^*, kPa	*E*, V	*I*, A/cm^2	*W*, W/cm^2	$p_s = c_s$	I_w, A/cm^2
101	0.78	0.015	0.012	0.146	0.132
	0.70	0.066	0.046	0.13	0.133
	0.60	0.192	0.116	0.09	0.136
	0.51	0.317	0.160	0.05	0.139
	0.37	0.409	0.151	0.02	0.142
	0.27	0.442	0.121	0.009	0.143
	0.21	0.454	0.094	0.005	0.143
505	0.80	0.014	0.011	0.17	0.078
	0.71	0.069	0.049	0.16	0.079
	0.60	0.286	0.172	0.12	0.081
	0.50	0.553	0.275	0.07	0.085
	0.40	0.709	0.281	0.04	0.087
	0.29	0.812	0.237	0.02	0.088
	0.20	0.863	0.176	0.01	0.088

the active layer and, as a consequence, to a significant decrease in the limiting currents of the cathode.

The negative effect of the elevated humidification of gases at the entrance to the gas chamber is successfully diminished by increasing the total pressure in the gas chamber. At $\varepsilon = 5$ ($p^* = 505$ kPa), the partial pressure of oxygen in the gas chamber now reaches the value of $p_0 = 0.833$, but the partial pressure of vapor in this case is only $p_{w0} = 0.167$ (at the boundary between the active and gas-diffusion layers at $t = 80$°C the partial pressure of vapor is now $p_{w1} = 0.093$). Therefore, curves *3* and *3'* in Fig. 4b become closer to curves *3* and *3'* in Fig. 3b. Although as a comparison of the data in Fig. 2b and Table 1 at the pressure $p^* = 505$ kPa and a cathode potential of $E = 0.5$ V shows, the overall current and specific power differ noticeably. In the absence of external diffusion restrictions in the gas-diffusion layer, $I = 3.6$ A/cm^2 and $W = 1.8$ W/cm^2, but with the presence of restrictions involving gas and vapor exchange, $I = 2.45$ A/cm^2 and $W = 1.22$ W/cm^2.

There is an even more noticeable decrease in the overall current and specific power with gases saturated with water vapor for the air cathode. Let us compare Figs. 3a and 4a and analyze the data in Table 2. At a pressure of $p^* = 101$ kPa in the gas chamber, the partial pressure of oxygen is now $p_0 = 0.033$ (in dry air $p_0 = 0.2$); the partial pressure of vapor is $p_{w0} = 0.83$; and the partial pressure of nitrogen is $p_{N0} = 0.137$. And again the situation moves in a better direction with an increase in the total pressure in the gas chamber. At $p^* = 505$ kPa in the gas chamber, the partial pressure of oxygen is $p_0 = 0.166$, already approaching the value of $p_0 = 0.2$. The partial pressure of vapor decreases significantly to $p_{w0} = 0.167$, and the partial pressure of nitrogen approaches its norm, $p_{N0} = 0.667$.

Thus, these findings confirm recommendations to raise the vapor temperature at the entrance to the gas chamber a somewhat: by 5°C for the oxygen or air cathode and by 10°C for the hydrogen anode [2]. If this recommendation is followed, then at $t = 85$°C (we will leave the temperature of the fuel cell at $t = 80$°C as before), the pressure of the vapor in the gas chamber is $p_{w1} = 56$ kPa. Then even at $p^* = 101$ kPa, the partial pressure of oxygen in the gas chamber will no longer be $p_0 = 0.163$ (as it was at a temperature of $t = 95$°C), but noticeably higher at $p_0 = 0.446$. If the cathode were operating at $t = 60$°C, then the choice of 65°C as the temperature of the saturated vapor (the pressure of the saturated vapor at this temperature is 25 kPa) would still be more favorable. Then even at $p^* = 101$ kPa, the partial pressure of oxygen in the gas chamber would be $p_0 = 0.75$.

Let us pay some more attention to the data in the last two columns of Tables 1 and 2. The penultimate column contains the partial pressure of oxygen p_s at the boundary between the active and gas-diffusion layers or, what is equal to it according to Henry's law, the reduced solubility of oxygen in Nafion c_s at this boundary. With a decrease in the cathode potential and an increase in the overall current, as already noted above, these quantities must decrease, and this, in the final analysis, causes the appearance of the limiting overall current.

Finally, let us turn to the last column in Tables 1 and 2. Values of I_w represent vapor flows in the gas-diffusion layer. They are positive when they move in the direction from the gas chamber to the active layer. These vapor flows are negative when they proceed from the active layer to the gas chamber as in the case when the temperature of the gas–vapor mixture at the entrance to the gas chamber is lower than the temperature of the fuel cell (conditions of drying in the active layer).

With a decrease in the cathode potential, vapor flows (data in Tables 1 and 2) change very little while the overall currents can increase by dozens of times. The calculations show that this pattern is also observed under conditions of drying in the active layer of the cathode. Thus, even under conditions of drying, when moisture is removed from the fuel cell, it is difficult to expect that vapor flows alone can achieve steady-state moisture exchange in the fuel cell with Nafion. Furthermore, significant differences between values of the overall current I and vapor flows I_w are observed in Tables 1 and 2. This also says that it is impossible to maintain moisture exchange in the fuel cell without the presence (which requires proper management) of liquid filtration in the pores of the gas-diffusion layer in the direction from the active layer to the gas chamber of the cathode.

CONCLUSIONS

The system of equations presented in this work allows us to calculate flows of gases and water vapor in the gas-diffusion layer. The calculation of the overall performance (overall current, specific power of the fuel cell, vapor flows, and the partial pressures of oxygen in the gas chamber and at the boundary between the active and gas-diffusion layers) of oxygen and air cathodes of a fuel cell with Nafion and platinum was carried out for three different cases: 1) when external restrictions on the oxygen supply to the active layer are completely absent, 2) when there are restrictions on the oxygen supply in the gas-diffusion layer, but flows of water vapor do not develop at all, and 3) when both gas and vapor exchange are present in the gas-diffusion layer. As a result of analyzing the results obtained by calculation, it was shown that the tendency to maintain the Nafion membrane in an optimal state (maximum proton conductivity without flooding the pores in the active layer of the cathode with moisture) by humidifying the membrane with vapor flows, which move from the gas chamber toward the active layer of the cathode, is accompanied by a significant decrease in the current and power characteristics of the fuel cell. It is possible to reduce these losses by decreasing the difference

between the temperature of the fuel cell and that of the saturated vapor in the gas chamber of the cathode and increasing the total pressure of the vapor–gas mixture in the gas chamber of the cathode.

NOTATION FOR PARAMETERS WHICH CHARACTERIZE THE GAS-DIFFUSION LAYER

p^* - total pressure of gases and water vapor in the gas chamber

p_0 - reduced partial pressure of oxygen in the gas chamber

p_s - reduced partial pressure of oxygen at the boundary between the active and gas-diffusion layers

p_{N0} - reduced partial pressure of nitrogen in the gas chamber

p_n - reduced partial pressure of nitrogen at the boundary between the active and gas-diffusion layers

p_{w0} - reduced partial pressure of water vapor in the gas chamber

p_{w1} - reduced partial pressure of water vapor at the boundary between the active and gas-diffusion layers

D^{**} - effective diffusion coefficient of the gas–vapor mixture

u^* - characteristic velocity of the movement of the gas–vapor mixture

I_d - characteristic diffusion current

$\bar{I}$ - reduced current generated in the active layer

$\bar{I}_w$ - reduced flow of water vapor

Δ - thickness of the gas-diffusion layer

τ - permeability of the gas-diffusion layer

μ - viscosity of air

α - ratio of the characteristic velocity of gas filtration to its diffusion velocity

NOTATION AND VALUES FOR PARAMETERS WHICH CHARACTERIZE THE ACTIVE AND GAS-DIFFUSION LAYERS OF THE CATHODE AND THE MEMBRANE

$t = 80°C$ - working temperature of the fuel cell

$E_{st} = 1.05$ V - steady-state cathode potential

$E^* = 0.825$ V - potential of the inflection point on the Tafel curve

$b_1 = 0.60\ V/2.3 = 2.6 \times 10^{-2}$ V - slope of the Tafel curve in the region of high potentials

$b_2 = 0.12\ V/2.3 = 5.2 \times 10^{-2}$ V - slope of the Tafel curve in the region of low potentials

$n = 4$ - number of electrons participating in the electrochemical process

$F = 9.6 \times 10^4$ C/mol - Faraday number

$i_o = 10^{-7}$ A/cm^2 - exchange current

$i^* = 8 \times 10^{-3}$ A/cm^3 - characteristic bulk current density in the region of high potentials

$D^* = 4.5 \times 10^{-4}$ cm^2/s - effective diffusion coefficient of oxygen in Nafion in the active layer

$c_o = 5 \times 10^{-6}\ \varepsilon$ g-mol/cm^3 - oxygen solubility in Nafion

$L = 100$ nm - average edge length of grains of Nafion and of the carrier

$d = 30$ nm - average dimension of pores in grains of the carrier

$g_e = 0.5$ - bulk concentration of Nafion grains

$g_s = 0.5$ - bulk concentration of grains of the carrier

$g_0 = 0$ - bulk concentration of "grains" of void space

$g_w = 20$ mass % - platinum content in grains of the carrier

$S^* = 1.33 \times 10^5$ cm^{-1} - specific contact surface between ionic and electron clusters

$S = 8 \times 10^4$ cm^{-1} - specific surface of platinum particles, which are available to participate in the electrochemical process

$I_d^* = 1.035$ A/cm^2 - characteristic diffusion current of the gas-diffusion layer

$\Delta = 100$ μm - thickness of the gas-diffusion layer

$\Delta_1 = 10$ μm - thickness of the active layer

$\Delta_2 = 10$ μm - thickness of the membrane

$\kappa = 1 \times 10^{-1}$ S cm^{-1} - specific conductivity of Nafion

$\kappa^* = 1.09 \times 10^{-2}$ S cm^{-1} - effective specific conductivity of Nafion in the active layer

$\nu = 0.5$ - porosity of grains of the carrier

$\xi = 0.6$ - catalytically active fraction of the surface of grains of the carrier

$\alpha^* = 0.156$ - ratio of characteristic velocity of gas filtration to its diffusion velocity

REFERENCES

1. Costamagna, P., and Srinivasan, S., *J. Power Sources*, 2001, vol. 102, pp. 253–269.
2. Ticianelli, E.A., Derouin, C.R., Redondo, A., and Srinivasan, S., *J. Electrochem. Soc.*, 1988, vol. 135, pp. 2209–2214.
3. Stefan, J., *Ann. Phys.,* 1882, vol. 17, pp. 550–560; 1890, vol. 41, pp. 725–747.
4. Frank-Kamenetskii, D.A., *Diffuziya i teploperedacha v khimicheskoi kinetike*, 3rd ed., Moscow: Nauka, 1987 [*Diffusion and Heat Transfer in Chemical Kinetics* (Engl. Transl. of 2nd Russ. Ed.), New York: Plenum, 1969].
5. Kheifets, L.I., and Neimark, A.V., *Mnogofaznye protsessy v poristikh sredakh* (Multiphase Processes in Porous Media), Moscow: Khimiya, 1982.
6. Mulder, M., *Basic Principles of Membrane Technology*, 2nd ed., Dordrecht: Kluwer, 1996.
7. Landau, L.D., and Lifshits, E.M., *Mekhanika sploshnykh sred*, Moscow: GITTL (State Publishing House of Technical-Theoretical Literature), 1954 [*Fluid Mechanics* (Engl. Transl.), Reading, Mass.: Addison-Wesley, 1959].

8. Damjanovic, A., Genshaw, M.A., and Bockris, J.O'M., *J. Chem. Phys.*, 1966, vol. 45, pp. 4057–4059.
9. Sepa, D.B., Vojnovic, V., and Damjanovic, A., *Electrochim. Acta*, 1981, vol. 26, pp. 781–793.
10. Parthasarathy, A., Srinivasan, S., Appleby, A.J., and Martin, C.R., *J. Electrochem. Soc.*, 1992, vol. 139, pp. 2856–2862.
11. Antoine, O., Bultel, Y., and Durand, R., *J. Electroanal. Chem.*, 2001, vol. 499, pp. 85–94.
12. Chirkov, Yu.G., and Rostokin, V.I., *Elektrokhimya*, 2006, vol. 42, pp. 806–812 [*Russ. J. Electrochem.* (Engl. Transl.), 2006, vol. 42, pp. 722–728].
13. Mitsushima, S., Araki, N., Kamiya, N., and Ota, K., *J. Electrochem. Soc.*, 2002, vol. 149, pp. A1370–A1375.
14. Parthasarathy, A., Srinivasan, S., Appleby, A.J., and Martin, C.R., *J. Electrochem. Soc.*, 1992, vol. 139, pp. 2530–2537.
15. Chirkov, Yu.G., and Rostokin, V.I., *Elektrokhimiya*, 2005, vol. 41, pp. 1109–1119 [*Russ. J. Electrochem.* (Engl. Transl.), 2005, vol. 41, pp. 985–995].
16. Uchida, M., Aoyama, Y., Eda, N., and Ohta, A., *J. Electrochem. Soc.*, 1995, vol. 142, pp. 4143–4149.
17. Chirkov, Yu.G., and Rostokin, V.I., *Elektrokhimiya*, 2004, vol. 40, pp. 1036–1048 [*Russ. J. Electrochem.* (Engl. Transl.), 2004, vol. 40, pp. 898–908].
18. Chirkov, Yu.G., and Rostokin, V.I., *Elektrokhimiya*, 2006, vol. 42, pp. 799–805 [*Russ. J. Electrochem.* (Engl. Transl.), 2006, vol. 42, pp. 715–721].
19. Gode, P., Lindbergh, G., and Sundholm, G., *J. Electroanal. Chem.*, 2002, vol. 518, pp. 115–122.
20. Chirkov, Yu.G., and Rostokin, V.I., *Elektrokhimiya*, 2007, vol. 43, pp. 27–35 [*Russ. J. Electrochem.* (Engl. Transl.), 2007, vol. 43, pp. 25–33].

SPELL: 1. Kamenetskii